Rictor/mTORC2 Is Essential for Maintaining a Balance Between β-Cell Proliferation and Cell Size

Yanyun Gu,[1,2] Jill Lindner,[1] Anil Kumar,[1,2] Weiping Yuan,[1] and Mark A. Magnuson[1,2]

OBJECTIVE—We examined the role of Rictor/mammalian target of rapamycin complex 2 (mTORC2), a key component of the phosphotidylinositol-3-kinase (PI3K)/mTORC2/AKT signaling pathway, in regulating both β-cell mass and function.

RESEARCH DESIGN AND METHODS—Mice with β-cell–specific deletions of *Rictor* or *Pten* were studied to determine the effects of deleting either or both genes on β-cell mass and glucose homeostasis.

RESULTS—*Rictor* null mice exhibited mild hyperglycemia and glucose intolerance caused by a reduction in β-cell mass, β-cell proliferation, pancreatic insulin content, and glucose-stimulated insulin secretion. Islets from these mice exhibited decreased AKT-S473 phosphorylation and increased abundance of FoxO1 and p27 proteins. Conversely, *Pten* null (β*Pten*KO) mice exhibited an increase in β-cell mass caused by increased cellular proliferation and size. Although β-cell mass was normal in mice lacking both *Rictor* and *Pten* (βDKO), their β-cells were larger than those in the β*Pten*KO mice. Even though the β-cell proliferation rate in the βDKO mice was lower than in the β*Pten*KO mice, there was a 12-fold increase the phosphorylation of AKT-T308.

CONCLUSIONS—PI3K/AKT signaling through mTORC2/pAKT-S473 plays a key role in maintaining normal β-cell mass. The phosphorylation of AKT-S473, by negatively regulating that of AKT-T308, is essential for maintaining a balance between β-cell proliferation and cell size in response to proliferative stimuli. ***Diabetes*** **60:827–837, 2011**

Pancreatic β-cell mass is adaptively regulated in response to factors such as glucose, insulin, IGF-1, placental lactogen, and glucoincretins, such as glucagon-like peptide 1 and gastric inhibitory polypeptide, all of which have been shown to have major roles in modulating β-cell mass (1–3). Signaling through the phosphotidylinositol-3-kinase (PI3K) pathway is essential for these stimuli to affect changes in β-cell mass. Prior studies have shown that an increase in PI3K signaling, induced either by the deletion of phosphatase and tensin homolog (*Pten*) (4) or by overexpressing AKT (5), leads to a marked expansion of β-cell mass. Conversely, an inhibition of PI3K signaling in β-cells, as achieved by genetic deletion of either insulin receptor substrate 2 (6) or phosphoinositide-dependent kinase 1 (PDK1) (7), dramatically reduces pancreatic β-cell mass.

From the [1]Center for Stem Cell Biology, Vanderbilt University Medical Center, Nashville, Tennessee; and the [2]Department of Molecular Physiology and Biophysics, Vanderbilt University Medical Center, Nashville, Tennessee.
Corresponding author: Mark A. Magnuson, mark.magnuson@vanderbilt.edu.
Received 22 August 2010 and accepted 1 December 2010.
DOI: 10.2337/db10-1194
This article contains Supplementary Data online at http://diabetes.diabetesjournals.org/lookup/suppl/doi:10.2337/db10-1194/-/DC1.

PI3K signaling is initiated by the production of phosphoinositide 3 (3,4,5)-phosphate (PI3P) from phosphoinositide 2 (4,5)-phosphate (PI2P) and attenuated by the dephosphorylation of PI3P back to PI2P by Pten (8,9). The accumulation of PI3P recruits AKT to the cell membrane where AKT can be activated by PDK1-mediated phosphorylation on a threonine (T) in the kinase domain (KD) (T308 in AKT2) and by mammalian target of rapamycin complex 2 (mTORC2)-mediated phosphorylation at a serine (S) in the hydrophobic motif (HM) (S473 in AKT2).

It has long been thought that the phosphorylation of T308 and S473 sites are additive with respect to AKT kinase activity, with the PDK1-dependent phosphorylation of T308 having a dominant role (10) over the mTORC2-dependent phosphorylation of S473. However, recent studies have shown that the site(s) at which AKT is phosphorylated may modify its specificity for downstream substrates. For instance, it has been shown that FoxO1/3a, in both mouse embryonic fibroblasts (11) and Drosophila S2 cells (12), can only be activated by mTORC2-dependent AKT-S473 phosphorylation. If extended to other cell types, differential downstream signaling by AKT could explain why PI3K signaling variably affects the size, proliferation, and metabolism of different cell types (8). In the case of the pancreatic β-cell, it is well known that PI3K/AKT signaling is essential for mediating changes in β-cell mass in response to growth factor/insulin signaling (13). However, it is not known whether the site-specific activation of AKT at either T308 or S473 has selective downstream effects.

To assess the role of AKT-S473 phosphorylation on PI3K signaling in the pancreatic β-cell, we deleted *Rictor*, a key component of mTORC2, thereby preventing phosphorylation of AKT at S473. Furthermore, to determine whether the site-specific activation of AKT at either T308 or S473 has selective downstream effects, or is negatively affected by feedback regulation (10), we explored the dynamics of signaling through both the KD and HM sites of AKT by simultaneously manipulating the expression of *Pten*. In this way, we were able to concurrently stimulate both PDK1 and mTORC2 activity. Our results indicate that phosphorylation of the KD and HM sites of AKT causes different effects on β-cell proliferation and size. In addition, we found that AKT-T308 phosphorylation is increased greatly by the loss of Rictor/mTORC2, suggesting the existence of a mechanism whereby the phosphorylation of AKT-S473 inhibits that of AKT-T308.

RESEARCH DESIGN AND METHODS

Animal maintenance and genotyping. Genotyping was performed by PCR using DNA extracted from ear or tail biopsies. The primers used for genotyping were as follows: $Rictor^{lox}$, 5′-ACTGAATATGTTCATGGTTGTG and 5′-GAAGTTATTCAGATGGCCCAGC; $PTEN^{lox}$, 5′-ACTCAAGGCAGGGATGAGC and 5′-GCCCCGATGCAATAAATA; *Ins2Cre*, 5′- CTCTGGCCATCTGCTGATCC and 5′-CGCCGCATAACCAGTGAAAC. To test the Cre-mediated recombination in *Rictor* or *Pten* in β-cells, genotyping was performed by PCR using DNA extracted from islets. The primers used for genotyping were as follows: *Rictor*,

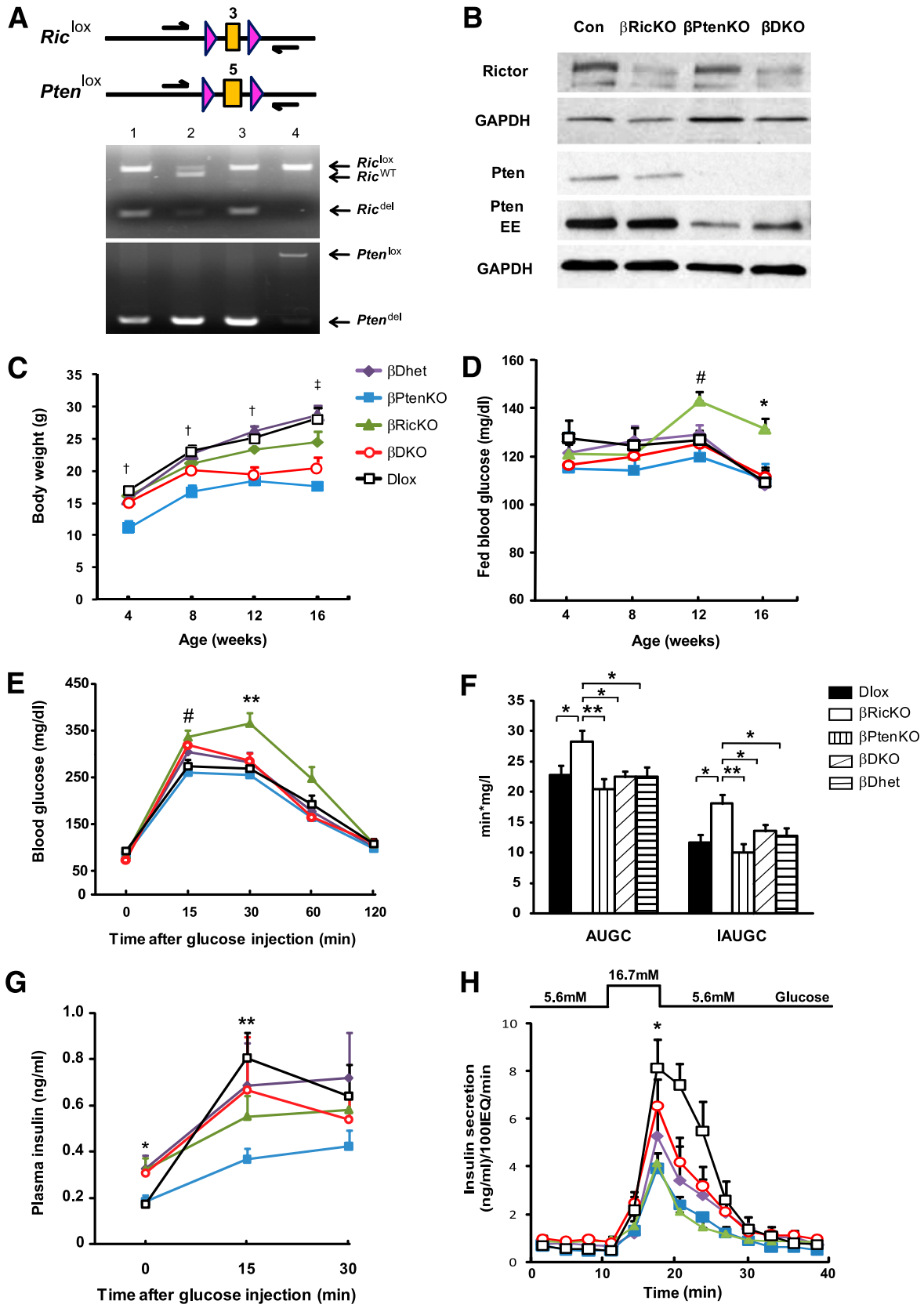

FIG. 1. Verification of tissue-specific deletion of *Rictor* or *Pten* and effects of Rictor or Pten deficiency on mouse growth and glucose metabolism. *A*: PCR analysis of islet DNA. *Upper*: Conditional *Rictor* and *Pten* alleles in which the LoxP sites are indicated by pink triangles. Expression of *Ins2Cre* results in the Cre-mediated deletion of exon 3 or 5 in the Rictor or Pten genes, respectively. *Lower*: Photographs of PCR analysis showing the loxed, wild-type, and deleted alleles of both genes (lane 1, β*Ric*KO, $Rictor^{lox/lox}$; $Pten^{lox/WT}$; $Ins2Cre^{+}$; lane 2, β*Pten*KO, $Rictor^{lox/WT}$; $Pten^{lox/lox}$; $Ins2Cre^{+}$; lane 3, βDKO, $Rictor^{lox/lox}$; $Pten^{lox/lox}$; $Ins2Cre^{+}$; and lane 4, D*lox*, $Rictor^{lox/lox}$; $Pten^{lox/lox}$). *B*: Western blot analysis of protein lysates isolated from control and mutant islets. Blots were probed with Rictor and Pten antibodies to verify the deletion of both genes. GAPDH was used as the loading control. *C*: Mouse body weight and fed blood glucose (*D*) were measured every 4 weeks between 4 and 16 weeks of age. †$P < 0.05$,

5′-ACTGAATATGTTCATGGTTGTG and 5′-GACACTGGATTACAGTGGCTTG; *Pten*, 5′-ACTCAAGGCAGGGATGAGC and 5′-CTTGATATCGAATTCCTGCAGC. Animal husbandry and experimentation were performed with approval of the Vanderbilt Institutional Animal Care and Use Committee under supervision of the Division of Animal Care. Mice were of a mixed genetic background of C57BL/6, BALB/c, and 129 strains.

Blood glucose and insulin assays. Mice were injected intraperitoneally with 2 mg dextrose/g body wt or 0.75 IU insulin/kg body wt (Novo Nordisk, Princeton, NJ) after an overnight or 6-h fast. Blood glucose concentrations were measured using a Logic Glucose Meter (Nova Biomedical, Waltham, MA). Plasma insulin values were determined by radioimmunoassay (Linco, St. Charles, MO).

β-Cell proliferation and cell size. Pancreata were isolated from embryos at embryonic day 17.5 and 3-month-old mice that were fed with water containing BrdU (0.08%, Sigma Aldrich, St. Louis, MO) for 1 week. Paraffin sections were labeled by anti-insulin, anti-BrdU, anti-Ki67, or anti-Glut2 antibodies (additional details in Supplementary Table 1). Insulin and BrdU or Ki67 double positive cells were counted as proliferating β-cells for each genotype (4,14) by Image J (National Institutes of Health, Bethesda, MD). β-Cell size was determined by measuring the internal area of islet cells as defined by Glut2 labeling using Metamorph version 7.1.0 (Molecular Devices, Sunnyvale, CA) (15).

β-Cell mass and insulin content. Pancreata were removed from 3-month-old mice, weighed, and then either embedded or homogenized. Paraffin tissue sections (every 250 μm, 5–15 sections per sample) were analyzed as previously described (15). Pancreatic homogenates were stored at −20°C until a radioimmunoassay for insulin concentration and protein assay (bicinchoninic acid assay, Thermo Fisher Scientific, Waltham, MA) were carried out for insulin content measurement.

Immunofluorescence and immunohistochemical staining. Antibodies used for immunochemistry are listed in Supplementary Table 1. Images were captured using a Zeiss Axioplan-2 upright microscope equipped with Q capture software (Molecular Devices, Sunnyvale, CA) or a Zeiss LSM 510 confocal microscope. Diaminobenzidine staining was performed using a diaminobenzidine peroxidase substrate kit (Vector Laboratories, Burlingame, CA).

Islet isolation and in vitro culture. Pancreata were digested by collagenase P, previously described for islet isolation (16). Isolated islets were then cultured overnight in Roswell Park Memorial Institute medium with 11.1 mmol/L glucose and 10% FBS. The next morning, they were washed and incubated in Roswell Park Memorial Institute medium with 5.6 mmol/L glucose and 0.5% BSA for an additional 4 h and then collected and stored at −80°C until analyzed (7).

Immunoblot analysis. Islet proteins were extracted, and protein concentration was determined using the BioRad DC reagent (Hercules, CA). For immunoblotting, islet extracts were subjected to SDS-PAGE before proteins were transferred electrophoretically to nitrocellulose membranes. Antibodies used for immunoblotting are listed in Supplementary Table 1. Densitometry quantification was performed with Image J.

RNA isolation and real-time quantitative RT-PCR. RNA from freshly isolated islets was extracted using Trizol (Invitrogen, Carlsbad, CA) and further purified with DNA-free kits (Zymo Research, Orange, CA). RNA concentration and integrity were determined using both a ND-1000 Spectrophotometer (NanoDrop, Wilmington, DE) and an Agilent Bioanalyzer (Agilent Technologies, Inc., Santa Clara, CA). cDNA was made using a High-Capacity cDNA Reverse Transcription Kit (Applied Biosystems, Carlsbad, CA). Real-time PCR was performed by custom-designed TaqMan Gene Expression Assay in a 7900HT Fast Real-Time PCR System (Applied Biosystems). The primer and probe sets used are listed in Supplementary Table 2.

Islet perifusion assay. Islets were placed in perifusion chamber at 37°C and perifused with Dulbecco's modified Eagle's medium at a rate of 1 mL/min (17). Islets were pre-equilibrated with media containing 5.6 mmol/L glucose for 30 min and then perifused with 5.6 mmol/L glucose for 10 min, 16.7 mmol/L glucose for 10 min, and 5.6 mmol/L glucose for another 20 min. Fractional insulin content was determined using a radioimmunoassay kit (Linco Research, St. Louis, MO). At the end of each perifusion study, the islets were collected and lysed with acid ethanol to measure total insulin content. The results are presented as insulin secreted normalized to 100 islet equivalents. The area under the curve was calculated for the interval between 10 and 30 min of perifusion.

β-Cell apoptosis. TdT-mediated X-dUTP nick-end labeling (TUNEL) was performed on serial pancreatic sections by using In Situ Cell Death Detection and Fluorescein kits (Roche, Basel, Switzerland). Cells were immunolabeled for insulin after TUNEL. Insulin and TUNEL double-positive cells within pancreatic islets were then counted and analyzed.

Statistical analysis. Statistical calculations were performed with SPSS 11.0 (SPSS Inc., Chicago, IL). Group comparisons were analyzed by Student *t* test and one-way ANOVA. Data are presented as mean ± SEM.

RESULTS

β-Cell–specific deletion of *Rictor* or *Pten* in mice. To eliminate the expression of *Rictor*/mTORC2 or *Pten* in a β-cell–specific manner, we intercrossed mice containing conditional *Rictor* (*Rictor*^{lox}) (18) or *Pten* alleles (*Pten*^{lox}) (4) with animals bearing an *Ins2Cre* transgene to generate mice that were null for *Rictor* (β*Ric*KO), null for *Pten* (β*Pten*KO), null for both *Rictor* and *Pten* (βDKO), heterozygous for both *Rictor* and *Pten* (βD*het*), or homozygous for both conditional alleles (D*lox*). Both βD*het* and D*lox* mice served as controls. To assess whether recombination was occurring in both the *Rictor*^{lox} and *Pten*^{lox} alleles, we performed PCR analysis using DNA extracted from islets and primers that flanked the recombination sites. As shown in Fig. 1*A*, DNA isolated from D*lox* islets showed no evidence of recombination in either allele, whereas DNA fragments of the predicted sizes were observed in both single and double allele knock-out (KO) mice. Although bands representing unrecombined alleles were seen in the β*Ric*KO, β*Pten*KO, and βDKO mice, they were likely due to the presence of non–β-cells in islets and incomplete recombination by the *Ins2Cre* transgene, as suggested by the detection of Cre in 56.2 ± 2% and 55.6 ± 3% of β-cells at embryonic day 17.5 and 12 weeks of age, respectively. Thus, to further confirm that the Cre-mediated recombination in *Rictor* and *Pten* reduces the expression of these proteins, we performed immunoblot analysis of protein lysates from isolated pancreatic islets. As shown in Fig. 1*B*, there was a reduction in the amount of both Rictor and Pten in islets containing the *Ins2Cre* transgene. Mice of all genotypes were viable and exhibited normal fertility; however, the growth rates of both the β*Pten*KO and βDKO mice differed from those of the other three genotypes (Fig. 1*C*), presumably as a result of the well-documented expression of the *Ins2Cre* transgene in the hypothalamus (4).

β*Pten*KO vs. other groups; ‡*P* < 0.05, β*Pten*KO and βDKO vs. other groups. #*P* < 0.05, β*Ric*KO vs. β*Pten*KO and D*lox*; **P* < 0.05, β*Ric*KO vs. all other groups. Purple diamonds, β*het* (*n* = 12–24); blue squares, β*Pten*KO (*n* = 7–20); green triangles, β*Ric*KO (*n* = 10–19); red circles, βDKO (*n* = 13–37); and black squares, D*lox* (*n* = 13–23). *E*: Intraperitoneal glucose tolerance test. Blood glucose concentrations were tested 0, 15, 30, 60, and 120 min after glucose injection. Blood glucose in β*Ric*KO mice was significantly higher than D*lox* at 15 and 30 min. βDKO mice had significantly improved blood glucose concentration compared with β*Ric*KO at 30 and 60 min. #*P* < 0.05, β*Ric*KO vs. β*Pten*KO and D*lox*; ***P* < 0.01, β*Ric*KO vs. all other groups, βD*het* (*n* = 13), β*Pten*KO (*n* = 7), β*Ric*KO (*n* = 15), βDKO (*n* = 9), and D*lox* (*n* = 13). *F*: AUGC and IAUGC were calculated following the trapezoid rule, to evaluate total blood glucose excursion after a glucose bolus. IAUGC was equal to AUGC minus the area beneath the fasting concentrations. β*Ric*KO mice had higher AUGC and IAUGC value than D*lox*. AUCG and IAUGC in βDKO mice showed significant improvement compared with β*Ric*KO. *G*: Curve of in vivo glucose-stimulated insulin secretion at 0, 15, and 30 min after glucose injection. Insulin secretion after peritoneal glucose injection in the β*Ric*KO mice trended lower at 15 min compared with the D*lox*. Insulin secretion between β*Ric*KO and βDKO mice showed no significant difference. β*Pten*KO mice had the lowest insulin secretion at 15 min after glucose bolus. **P* < 0.05, β*Pten*KO and D*lox* vs. all other groups; ***P* < 0.05, β*Pten*KO vs. all other groups, βD*het* (*n* = 13), β*Pten*KO (*n* = 7), β*Ric*KO (*n* = 15), βDKO (*n* = 9), and D*lox* (*n* = 13). *H*: Curve of insulin secretion per 100 islet equivalents in ex vivo perifusion test in all genotypes. Isolated islets were incubated with 5.6 mmol/L and 16.7 mmol/L glucose, and insulin secretion was measured every 3 min up to 42 min (*n* = 3). **P* < 0.05, β*Ric*KO and β*Pten*KO vs. D*lox*; ***P* < 0.01, β*Ric*KO and β*Pten*KO vs. D*lox*. All data presented as mean ± SEM. EE, extended exposure. (A high-quality digital representation of this figure is available in the online issue.)

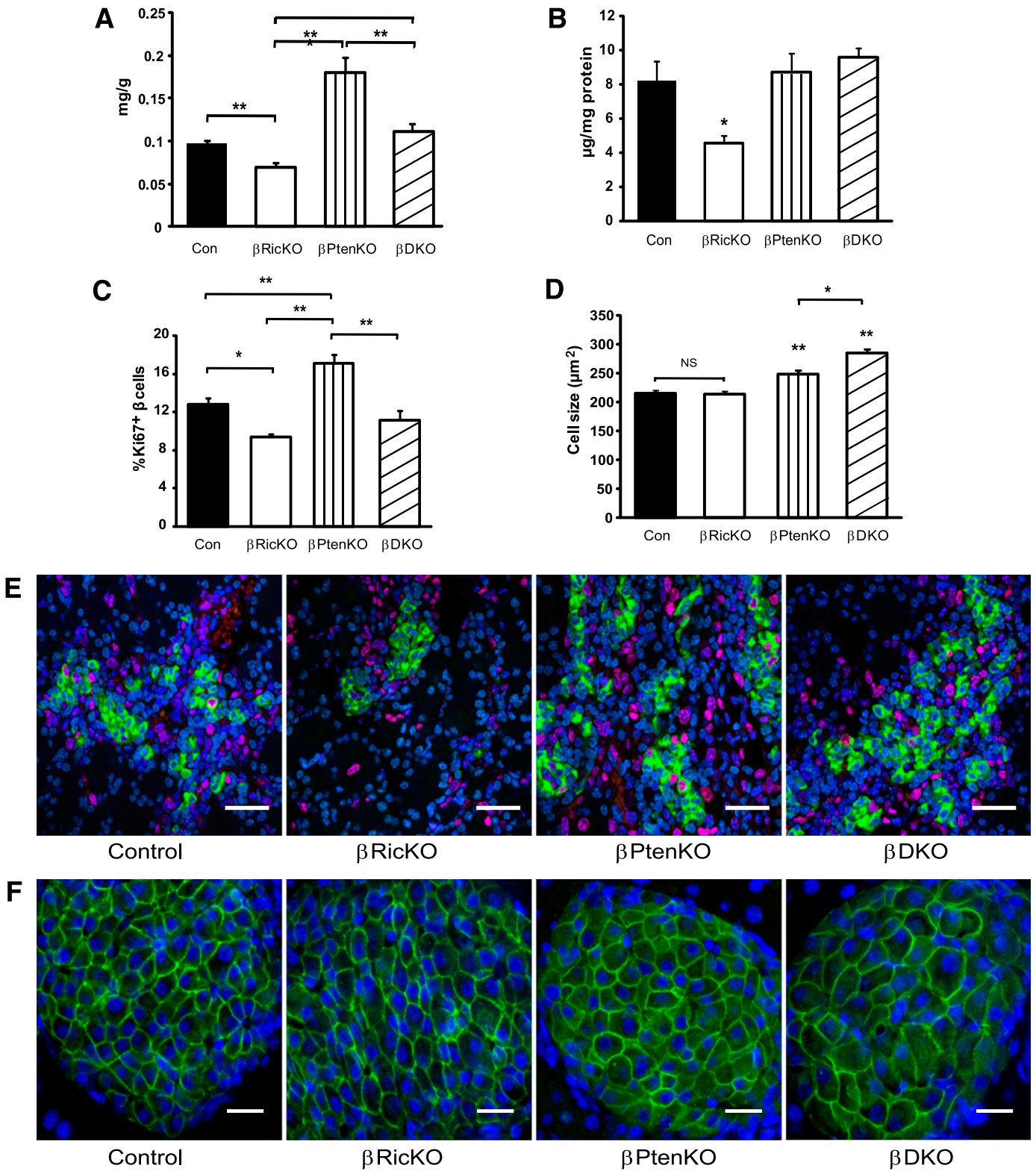

FIG. 2. Effects of Rictor or Pten deficiency on pancreatic islet characteristics and insulin content. Paraffin sections from 3-month-old mice were immunolabeled with insulin and BrdU, Ki67, or Glut2. *A*: β-Cell mass adjusted for body weight. β*Pten*KO mice showed higher β-cell mass when compared with other groups. β*Ric*KO showed a significantly reduced β-cell mass compared with control group. **P* < 0.05; ***P* < 0.01. *B*: Whole pancreatic insulin content was compared among all the groups. β*Ric*KO showed the lowest insulin content among all genotypes. **P* < 0.05. *C*: Quantification of the percentage of β-cells labeled for both Ki67 and insulin. β*Ric*KO had lowest percentage of double-labeled cells. At least 1,000 cells from three embryonic pancreata were counted for each genotype to determine the number of insulin positive and insulin/Ki67 double-positive cells. **P* < 0.05; ***P* < 0.01. *D*: Quantification of β-cell size. βDKO had largest cell size compared with other groups. In all cases, three to five mice per genotype were analyzed. In total, 500–1,000 cells were counted, and there were at least three animals per group. **P* < 0.05 vs. all other groups or between indicated groups. ***P* < 0.01 vs. all other groups or between indicated groups. Data presented as mean ± SEM. *E*: Representative immunolabeled sections from embryonic day 17.5 pancreata for insulin (green), Ki67 (red), and Topo3 (blue) nuclear staining. Insulin/Ki67 immunolabeling in pancreatic islets was used to identify proliferating β-cells. Scale bar = 20 μm. *F*: Representative immunolabeled sections of pancreas from adult mice for Glut2 (green) and DAPI (blue) nuclear staining. Glut2 was used to label the β-cell membrane to measure cell size. Scale bar = 25 μm. (A high-quality digital representation of this figure is available in the online issue.)

Effects of deleting *Rictor* or *Pten* on glucose metabolism and insulin secretion. To assess the effects of the absence of Rictor/mTORC2 or Pten in β-cells on glucose metabolism, we first determined the fed blood glucose concentration in mice between 4 and 16 weeks of age. The β*Ric*KO mice exhibited hyperglycemia beginning at 12 weeks (Fig. 1*D*), whereas the blood glucose concentrations of the βDKO mice remained similar to those of the controls. Insulin sensitivity assessed by insulin tolerance test at 12 weeks did not differ among the four groups of mice (Supplementary Fig. 1*A* and *B*). The β*Ric*KO mice, compared with both the D*lox* and βD*het* mice, showed slower glucose clearance as indicated by elevated blood glucose concentrations at 15 and 30 min after an intraperitoneal glucose bolus. Total glucose excursion, calculated by both the area under glucose curve (AUGC) and increment AUGC (IAUGC), were significantly higher in the β*Ric*KO mice compared with the D*lox* and βD*het* animals (Fig. 1*E* and *F*). Conversely, the βDKO mice showed a significantly lower blood glucose concentration at 30 and 60 min, and lower AUGC and IAUGC values, compared with the β*Ric*KO mice. In addition, despite their higher blood glucose concentrations, the β*Ric*KO mice had lower plasma insulin levels 15 min after glucose challenge (Fig. 1*G*), and lower total insulin output calculated by AUIC and IAUIC (Supplementary Fig. 1*C*), compared with the D*lox* and βD*het* mice. The βDKO mice showed a trend toward higher insulin secretion compared with β*Ric*KO animals, but these differences were not significant. Both the D*lox* and βD*het* control groups showed similar glucose tolerance and insulin secretion ability. To confirm an insulin secretory defect in β*Ric*KO mice, we performed islet perifusion experiments. As shown in Fig. 1*H* and Supplementary Fig. 1*D*, islets from β*Ric*KO mice had approximately 70% lower insulin secretion in response to 16.7 mmol/L glucose than the D*lox* islets. Conversely, insulin secretion by the glucose-stimulated βDKO islets was increased to a level similar to that of D*lox* islets (Fig. 1*H* and Supplementary Fig. 1*D*).

Effects of deleting *Rictor* or *Pten* on β-cell insulin content and mass. Because the impaired insulin secretion could be due to lower β-cell mass or inadequate insulin production, we analyzed the mice for changes in β-cell mass and insulin content (Fig. 2*A* and *B*). To take into account the growth retardation of both β*Pten*KO and βDKO mice at 12 weeks of age, β-cell mass was normalized by the body weight of the animal (Fig. 2*A* and Supplementary Fig. 2). The adjusted β-cell masses of the β*Ric*KO and β*Pten*KO mice were 28% lower ($P < 0.01$) and 86% higher ($P < 0.01$), respectively, than the controls. Moreover, β-cell mass in the βDKO mice was approximately 40% lower than that of the β*Pten*KO animals ($P < 0.05$). The pancreatic insulin content of the β*Ric*KO animals was ~50% less than the control mice but was unchanged in both the β*Pten*KO and βDKO animals (Fig. 2*B*).

Effects of deleting *Rictor* on β-cell proliferation and size. To determine whether a change in the number or size of β-cells was responsible for the changes in β-cell mass, we also measured β-cell proliferation and cell size. Because of the very low β-cell turnover in adult mice (14), β-cell proliferation was assessed by measuring the percentage of Ki67-positive β-cells at both embryonic day 17.5, a period when β-cells undergo a burst of cell proliferation (19,20), and 12 weeks. As shown in Fig. 2*C* and *E* and Supplementary Fig. 3, the number of proliferating β-cells decreased 26% in the β*Ric*KO mice and increased 34% in the β*Pten*KO mice compared with the controls ($P < 0.05$), whereas the βDKO mice did not show increased β-cell proliferation, as was seen in the β*Pten*KO mice. Islet number per pancreatic unit area was unchanged in the β*Ric*KO mice (data not shown).

Because AKT is known to mediate antiapoptotic effects, we also assessed whether the loss of Rictor/mTORC2 in β-cells might lead to an increase in apoptosis. However, as shown in Supplementary Fig. 4, there was no increase in apoptosis in Rictor null β-cells when compared with control cells as determined by TUNEL staining.

The average β-cell size, shown in Fig. 2*D* and *F*, which was unaffected in the β*Ric*KO animals, was increased by 15% in the β*Pten*KO animals. Surprisingly, the average β-cell size was increased by 31% in βDKO mice, which in turn was 15% larger than that of the β*Pten*KO mice ($P < 0.05$). The measurements of both β-cell proliferation and cell size, as summarized in Table 1, suggest that the lack of *Rictor*/mTORC2 in β-cells leads to a reduction in β-cell mass mainly because of a decrease in β-cell proliferation.

mTORC2 is required for the activation of AKT via S473 and signaling to downstream targets. To examine whether AKT and its substrates transduce a proliferative signal from mTORC2, we analyzed the phosphorylation of AKT and FoxO1 and p27 protein levels in islet protein extracts (Fig. 3). The phosphorylation of AKT at S473 in β*Ric*KO islets was diminished 70% compared with the controls (Fig. 3*A* and *B*). We also found that the amount of FoxO1 and p27 was approximately 1.5-fold greater than the control in β*Ric*KO islets (Fig. 3*C* and *D*). These findings suggest that the reduction in AKT-S473 phosphorylation, caused by the loss of mTORC2, leads to an increase in cellular abundance of both FoxO1 and p27. The accumulation of these proteins in β*Ric*KO β-cells would be expected to reduce β-cell proliferation by slowing cell cycle progression (21,22).

Ablation of both Rictor/mTORC2 and Pten increases phosphorylation of AKT T308. Having confirmed a reduction in AKT-S473 phosphorylation in the absence of Rictor/mTORC2 and alterations in downstream targets for AKT signaling, we next sought to determine whether the

TABLE 1
Changes in β-cell mass, proliferation, and size in the mice used in this study compared with the changes previously observed in β*PDK1*KO mice

	β*PDK1*KO vs. control (7)	β*Pten*KO vs. control	β*Ric*KO vs. control	βDKO vs. control	βDKO vs. β*Pten*KO
β-Cell mass	↓80%	↑86%	↓28%	–	↓40%
β-Cell proliferation	↓50%	↑34%	↓26%	–	↓35%
β-Cell size	↓20%	↑15%	–	↑30%	↑15%

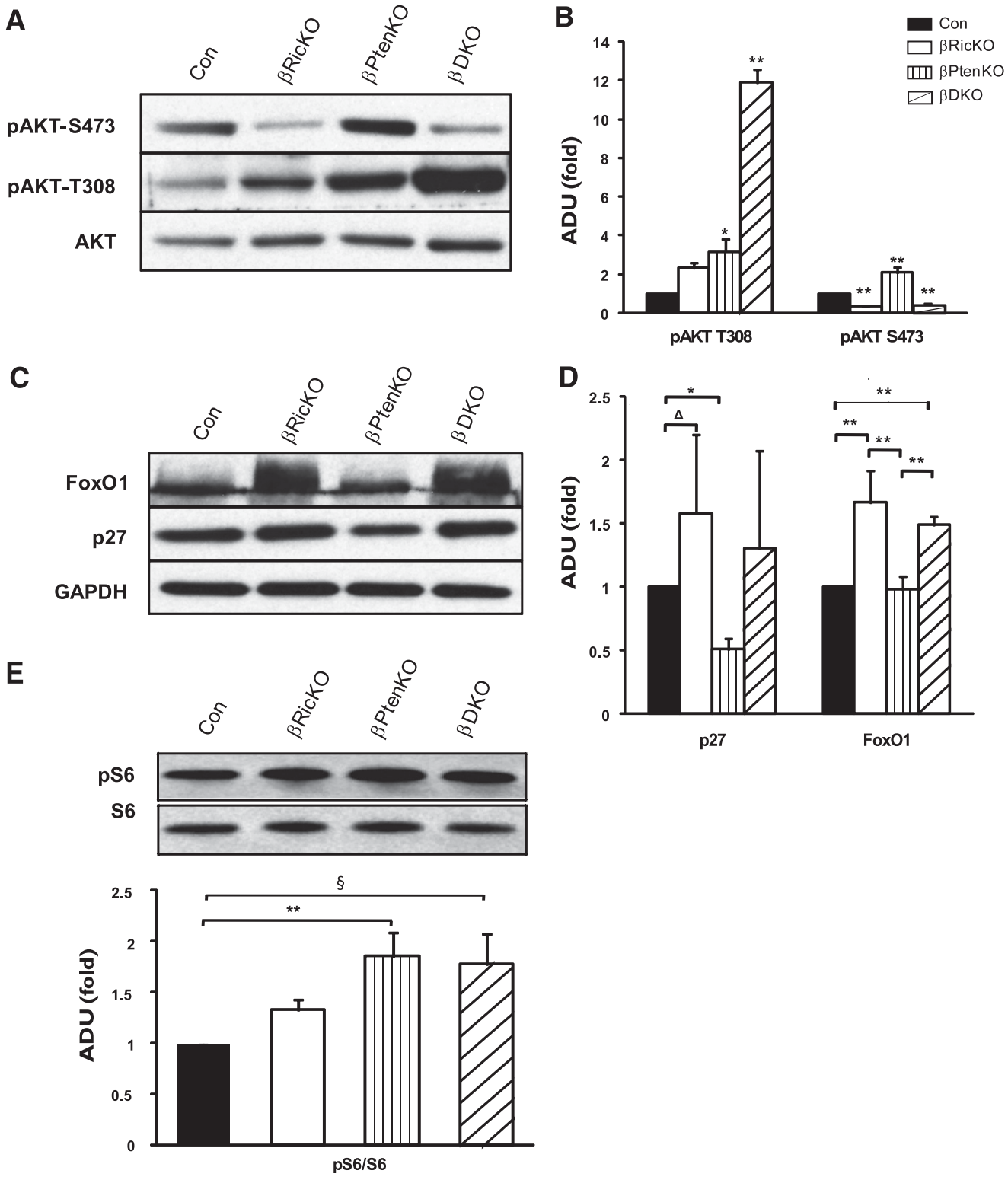

FIG. 3. Western blot and densitometry analysis of islet proteins in different genotypes. *A*: Western blotting for determining total and phosphorylated AKT. The phosphorylation of AKT at T308 and S473, and total AKT protein were examined in islets of mutant and control groups. *B*: Densitometry analysis for AKT phosphorylation. *C*: Immunoblot of p27 and FoxO1 using GAPDH as a loading control. *D*: Densitometry analysis for p27 and FoxO1 protein adjusted with GAPDH. *E*: Immunoblot for phosphorylation of S6 (*top*) and densitometry analysis (*bottom*). Figures represent blots from multiple mice in each genotype. Results are presented as relative folds of change in mutant compared with control mice. Control is D*lox*. *$P < 0.05$ vs. all other groups or the indicated group; **$P < 0.01$ vs. all other groups or indicated group; §$P = 0.07$. Four to five mice were studied per groups. Data are presented as mean ± SEM. ADU, arbitrary density unit.

phosphorylation of these target proteins was also altered in response to the increased PI3K signaling brought about by the deletion of *Pten*. The absence of Pten alone in the β-cell (β*Pten*KO mice) resulted in an increase in both pAKT-S473 (2.1-fold) and pAKT-T308 (3.2-fold) compared with the controls (Fig. 3*A* and *B*). However, in the βDKO mice, pAKT-S473 was decreased to the same low level seen in the β*Ric*KO mice. Surprisingly, the phosphorylation of AKT-T308 in the βDKO mice was 11.8-fold higher than that of the controls ($P < 0.01$), greatly exceeding the 3.7-fold increase observed in the β*Pten*KO animals ($P < 0.01$).

Downstream targets of AKT were also significantly affected by the loss of Rictor or Pten. Specifically, the amount of p27 was decreased by 50% in β*Pten*KO islets but increased in the βDKO mice to a level similar to that of the controls (Fig. 3*C* and *D*). Similarly, the amount of FoxO1 was normal in β*Pten*KO islets but significantly increased in the βDKO mice. Other signaling downstream of AKT, such as S6 phosphorylation (Fig. 3*E*), which is mediated through mTORC1, was increased in both β*Pten*KO ($P < 0.05$) and βDKO islets ($P = 0.07$). These data indicate that in pancreatic β-cells the phosphorylation of AKT-S473 is dependent on Rictor/mTORC2 signaling. Notably, the increased phosphorylation of AKT-T308 that occurs with the loss of Rictor/mTORC2 in βDKO suggests that either Rictor/mTORC2 itself or a downstream target of pAKT-S473 has an inhibitory effect on the PDK1-mediated phosphorylation of AKT-T308.

Ablation of both Rictor/mTORC2 or Pten changes FoxO1 cellular distribution. On phosphorylation by AKT, FoxO1, which normally resides in the nucleus where it inhibits β-cell proliferation, enters the cytoplasm where it is ubiquitinated and degraded (22,23). Thus, to determine whether FoxO1 cellular distribution was affected by the absence of Rictor or Pten in β-cells, we studied the subcellular localization of FoxO1 in β-cells (Fig. 4 and Supplementary Fig. 5). As expected, FoxO1 was mostly located in nuclei of β-cells of control mice (Fig. 4*A* and *E*). Moreover, in the β*Ric*KO mice nuclear FoxO1 levels were further increased (Fig. 4*B* and *F* and Supplementary Fig. 5) compared with D*lox* β-cells. However, FoxO1 was shifted almost entirely to the cytoplasm in the β*Pten*KO mice (Fig. 4*C* and *G* and Supplementary Fig. 5). In βDKO mice (Fig. 4*D* and *H* and Supplementary Fig. 5), the nuclear localization of FoxO1 in β-cells was restored. Similarly, islets from β*Ric*KO mice also showed diminished nuclear Pdx1 labeling (Supplementary Fig. 6), whereas βDKO islets maintained a normal nuclear localization pattern. These findings suggest that the mTORC2-dependent phosphorylation of AKT-S473 regulates FoxO1 activity by changing its cellular distribution and that this regulation is independent of the increased phosphorylation of AKT-T308 in *Pten* null pancreatic β-cells.

***Rictor* or *Pten* deletion alters the gene expression profile of many pancreatic genes.** To explore the consequences on gene expression of deleting *Rictor* or *Pten* in β-cells, we assessed the mRNA transcriptional profiles of 43 genes in pancreatic islets from β*Ric*KO, β*Pten*KO, and βDKO mice as shown in Fig. 5*A*. Among genes that regulate cell cycle progression, we found that the expression of *p27* was decreased by approximately 50% in the β*Pten*KO mice, *CDK4* was decreased 25% in the β*Ric*KO group, and *p21* was increased in all mutant mice, and was most highly expressed in the β*Pten*KO animals. These changes were partially (*p27* and *p21*) or totally restored (*CDK4*) in the βDKO mice (Fig. 5*B*). Among genes that play a role in insulin

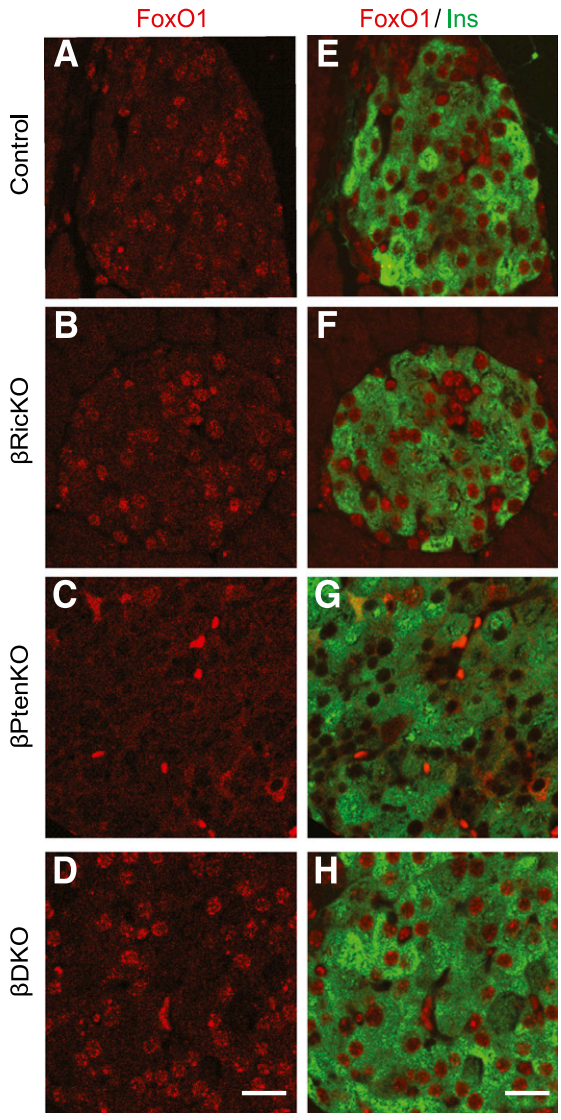

FIG. 4. Differential cellular distribution of FoxO1 in pancreatic β-cells with different genotypes. *A–D*: Immunolabeling of FoxO1 (red) in pancreatic islets. *E–H*: Double immunolabeling of FoxO1 (red) and insulin (green). *A* and *E*: FoxO1 immunolabeling in control islets showing its localization mainly in the nucleus. *B* and *F*: FoxO1 immunolabeling in β*Ric*KO islets. β*Ric*KO islets showing a more intense nuclear FoxO1 staining than the controls. *C* and *G*: FoxO1 immunolabeling in β*Pten*KO islets showing the lack of nuclear FoxO1 accumulation. *D* and *H*: FoxO1 immunolabeling in βDKO islets. Nuclear staining pattern in βDKO islets is similar to β*Ric*KO islets. Scale bar = 20 μm. (A high-quality digital representation of this figure is available in the online issue.)

secretion, *Connexin-36* (24,25) and *Vamp-2* (26) were diminished in the β*Ric*KO mice. In contrast, *Syntaxin-1* (26) was unaffected in the β*Ric*KO mice but increased in βDKO β-cells (Fig. 5*C*). Despite unchanged *Pdx1* expression, the expression of *MafB* was elevated in both the β*Ric*KO and βDKO mice, and *Neurog3* was increased in β*Ric*KO animals (Fig. 5*D*).

DISCUSSION

Mice lacking β-cell Rictor/mTORC2 exhibit impaired glucose tolerance due to a combination of reduced pancreatic insulin content and impaired glucose-stimulated insulin secretion. The reduced pancreatic insulin content is due to a lower β-cell mass brought on by diminished rates of

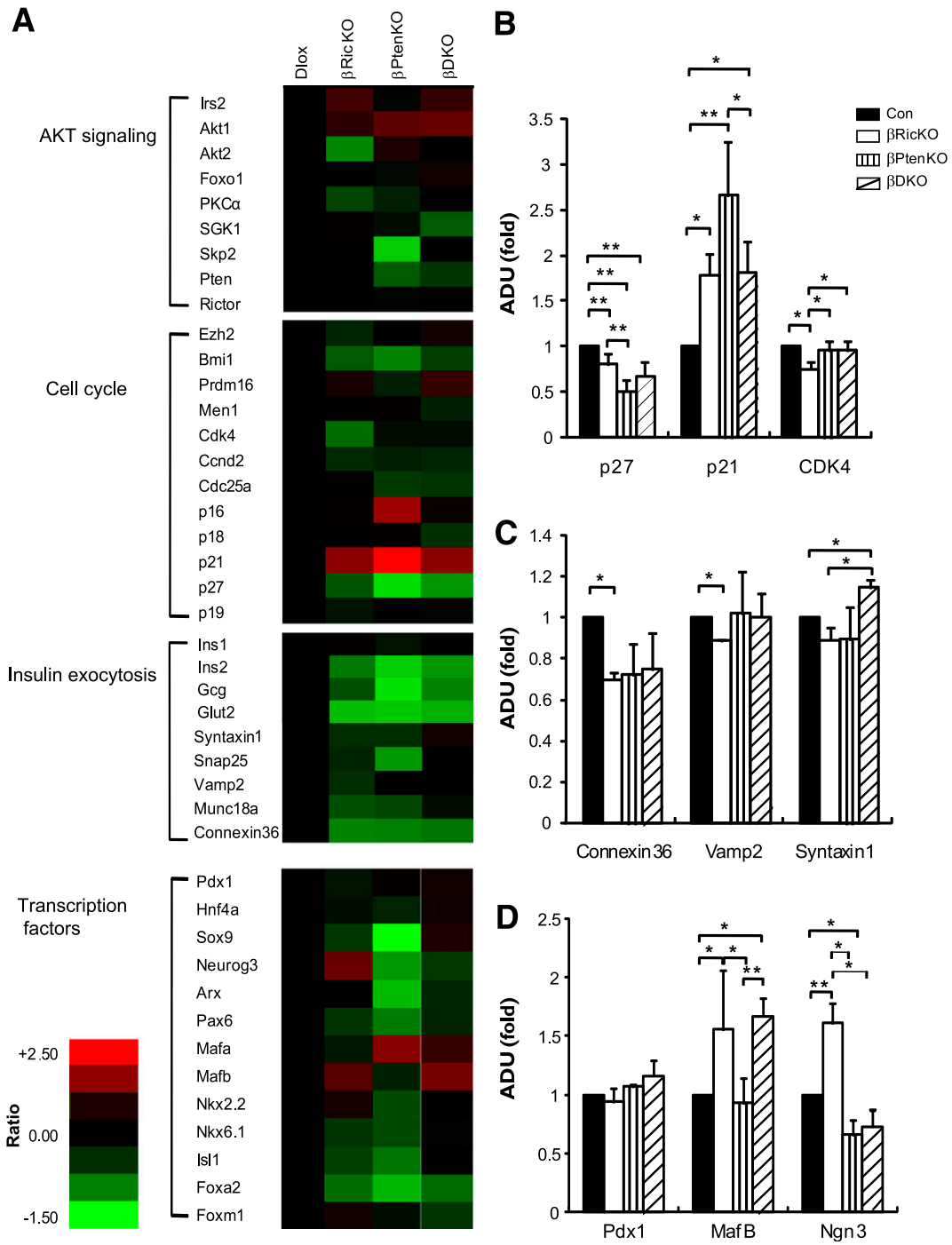

FIG. 5. Deletion of *Rictor* or *Pten* changed gene expressions of pancreatic transcription factors and genes related to cell cycle and insulin secretion in pancreatic islets. *A*: Heat map representing comparison of gene expression profile determined by *TaqMan* RT-PCR and calculated by -ΔΔCT method with 18S RNA as the internal control. A total of 43 genes from the four categories indicated on the far left were analyzed. Gene expression abundance was shown in varying color levels of red and green, with red representing upregulation, green representing downregulation, and black representing the level in the control group. *B*: Comparisons of some cell cycle-related genes: *p27*, *CDK4*, and *p21* expression profiles were significantly different among all genotypes. *C*: Comparison of genes regulating insulin secretion machinery; *Vamp-2*, *Connexin-36*, and *Syntaxin-1* had differential gene expression patterns in all four genotypes. *D*: Comparisons of critical pancreatic transcription factors; *Pdx1*, *MafB*, and *Neurog3* showed differential expression patterns in all four genotypes. Control is D*lox*. *$P < 0.05$; **$P < 0.01$. Data are presented as mean ± SEM. Three mice were analyzed for each genotype.

β-cell proliferation, not an increase in β-cell apoptosis. At a molecular level, the absence of Rictor/mTORC2 impairs PI3K signaling through AKT by blocking the phosphorylation of AKT at S473. This leads to a reduction in AKT activity, thereby suppressing cell division, by both activating p27 and increasing the accumulation of FoxO1 in the nucleus.

The loss of mTORC2-mediated phosphorylation of AKT seems to have less of an impact on β-cell proliferation than does the loss of PDK1 (7), as summarized in Table 1, although this is difficult to accurately assess between the different studies. Our findings indicate that signaling through mTORC2/pAKT-S473 promotes β-cell proliferation

in a manner that is independent of PDK1/pAKT-T308. Indeed, the lack of Rictor/mTORC2 resulted in lower rates of both β-cell proliferation, even in the presence of a 12-fold increase in pAKT-T308, as occurs in the βDKO mice. Thus, mTORC2-mediated phosphorylation of AKT-S473 clearly contributes to the maintenance of β-cell mass, even if quantitatively less than that of PDK1/pAKT-T308.

Rictor/mTORC2 is also important for normal β-cell function, as shown by approximately 70% reduction in glucose-stimulated insulin secretion β*Ric*KO islets. The reduced insulin secretion is likely due to impaired insulin biosynthesis because there was a 50% reduction in pancreatic insulin content (Fig. 2*B*) but only a 30% decrease in β-cell mass (Fig. 2*A*). However, insulin exocytosis also seems to be impaired. Consistent with this are *1*) the cytoplasmic translocation of Pdx1 (Supplementary Fig. 6), *2*) the nuclear accumulation of FoxO1 in β*Ric*KO islets (Fig. 4 and Supplementary Fig. 5), and *3*) the impaired expression of several genes involved in insulin exocytosis, such as *Vamp-2* and *Connexin-36* (Fig. 5*C*). Pdx1 is an important determinant of β-cell function that is known to be regulated by PI3K/ATK signaling (23,27,28). It is also a direct downstream target of FoxO1 (22). Indeed, at least two prior studies have shown that PI3K/AKT signaling stimulates insulin biosynthesis and secretion (5,29). Thus, our study provides additional evidence that Rictor/mTORC2 is important for the PI3K-mediated regulation of β-cell function via the previously reported AKT/FoxO1/Pdx1 pathway (22,23,27,28).

The phenotype of the βDKO mice, although complex, was highly informative. Although the near reversal in the βDKO mice of the impairments of β-cell proliferation and insulin secretion observed in the β*Ric*KO mice might have been expected, we were surprised to find that the β-cells of βDKO mice were larger in size than the other genotypes. Although we only assessed changes in β-cell area, our measurements predict an even larger increase in the actual volume of these cells. The increase in cell size correlates with an ~12-fold increase in pAKT-T308 in the βDKO mice, more than the increase in both β-cell size and AKT-T308 phosphorylation in the β*Pten*KO animals. Thus, we propose that the marked increase in AKT-T308 phosphorylation that occurs in the absence of Rictor/mTORC2 is caused by the disruption of a negative feedback loop that is essential for maintaining normal-sized β-cells.

The simultaneous reduction in β-cell proliferation and enlargement of β-cells in the βDKO mice, compared with β*Pten*KO mice, is most easily explained if the two phosphorylation sites in AKT have different downstream effects. Indeed, our findings and those of others (7) are consistent with pAKT-S473 principally affecting the rate of β-cell proliferation and pAKT-T308 mainly affecting β-cell size. Our analysis of downstream signaling events revealed that the changes in β-cell proliferation were correlated with alterations in pAKT-S473, FoxO1, and p27. Both FoxO1 and p27 protein amount, and FoxO1 nuclear localization were increased in the βDKO mice, even though these mice have an ~12-fold elevation of pAKT-T308 and are consistent with previous studies showing that pAKT-S473 exclusively activates FoxO1 signaling (11,12). Because both FoxO1 and p27 are negatively regulated by AKT, and both serve as critical cell cycle inhibitors for pancreatic β-cells (30,31), the increased amount of these proteins in the β*Ric*KO mice would be expected to cause a reduction in β-cell proliferation, and thus mass.

Similarly, the notion that pAKT-T308 may regulate β-cell size is supported by other studies demonstrating that the deletion of PDK1 in various tissues (7,32–36), as well as the whole embryo (37), both impairs mTORC1/S6 signaling and lowers cell size despite a reciprocal increase in pAKT-S473. A role for AKT/mTORC1 signaling in the regulation of β-cell size has clearly been shown in studies in which mTORC1/S6 signaling has been augmented, either by deleting TSC1/TSC2 (38) or by overexpressing Rheb (39). Although we found an increase of pS6 in both βPtenKO and βDKO cells, the increment of pS6 was less than that of pAKTS308, suggesting other downstream signaling of pAKT-T308 or mTORC1 might also contribute to cell size regulation.

When prior studies are considered (40), our findings are consistent with the existence of dual, reciprocal feedback signaling loops involving AKT (Fig. 6) that, together, function to maintain a tight balance between cell proliferation

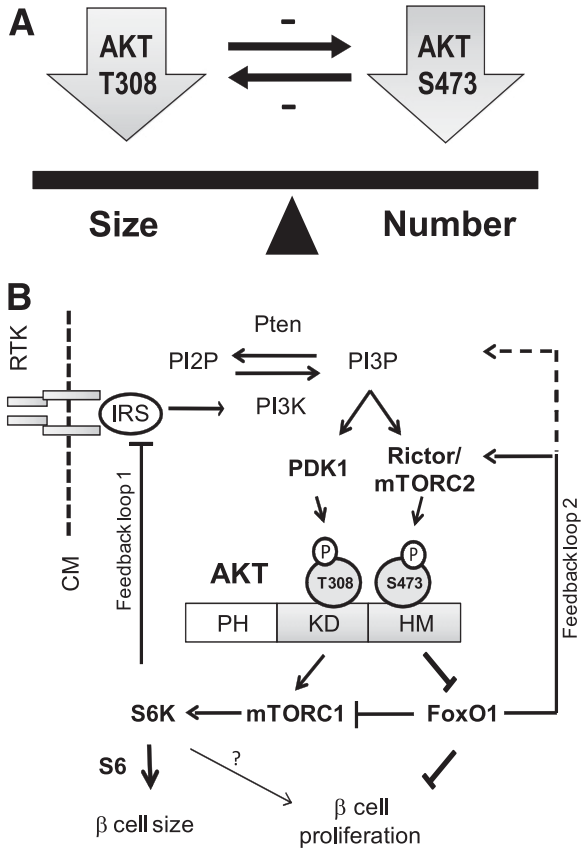

FIG. 6. Model for the differential roles of the two AKT phosphorylation sites in regulating pancreatic β-cell size and proliferation. *A*: Balance between β-cell size and cell number is maintained by the site-specific phosphorylation of AKT at T308 and S473 and dual negative feedback loops. *B*: PI3K/AKT signaling is activated by growth factors/insulin binding to their receptors. In the case of insulin, insulin receptor activation stimulates insulin receptor substrate, which then activates PI3K and phosphorylation of PI2P to PI3P. The intracellular accumulation of PI3P then stimulates PDK1 and mTORC2 to phosphorylate AKT at T308 and S473, respectively. AKT is phosphorylated at both T308 and S473. Phosphorylation of AKT-T308 (pAKT-T308) selectively targets mTORC1/S6, whereas phosphorylation of AKT-S473 (pAKT-S473) selectively targets FoxO1/p27 signaling. These AKT phosphorylations mutually regulate to maintain β-cell mass homeostasis. Solid arrows indicate the known signaling events; dashed lines indicate a newly proposed inhibitory feedback mechanism. CM, cell membrane; IR, insulin receptor; IRS, insulin receptor substrate; PH, pleckstrin homology domain.

and cell size (Fig. 6*A*). In this model (Fig. 6*B*), pAKT-T308 causes a negative feedback inhibition on pAKT-S473 and, reciprocally, mTORC2/pAKT-S473 signaling inhibits pAKT-T308. Although signaling through pAKT-T308 to mTORC1 may explain how the first feedback loop is mediated (10,40), the mechanism whereby pAKT-S473 signals to FoxO1 to inhibit pAKT-T308 is less certain. We suggest that the upregulation of FoxO1, which occurs in the Rictor-null β-cells, releases an inhibition of PI3K/PDK1/pAKT-T308 signaling. If so, this would position FoxO1 as a positive regulator of PI3K/PDK1/pAKT-T308. However, because FoxO1 has not been demonstrated to play any role in the regulation of PI3K/PDK1/pAKT-T308 in β-cells, this possibility, for the time being, is speculative.

In any case, although some aspects of this model are unproven, it provides an appealing explanation for our findings and suggests mechanisms whereby the site-specific phosphorylation of AKT may exert differential effects on β-cell proliferation and cell size. In this model (Fig. 6*B*), the increase in pAKT-S473 causes the downregulation of both FoxO1 and p27, which, through inhibition of PI3K/PDK1/pAKT-T308, induces cell proliferation. Conversely, an increase in pAKT-T308, brought about by the upregulation of FoxO1 and p27, slows cell proliferation and stimulates an expansion in the size, or cellular hypertrophy, of β-cells. Thus, by exerting distinct downstream signaling effects in response to phosphorylation at either T308 or S473, AKT serves as a focal point for maintaining a balance between β-cell proliferation and cell size in response to stimuli that increase β-cell mass.

ACKNOWLEDGMENTS

This study used the Vanderbilt Cell Imaging, Islet Procurement and Analysis, and Hormone Assay Cores, which are supported by National Institutes of Health Grants CA-68485, DK-20593, DK-58404, HD-15052, DK-59637, and EY-08126. This work was further supported by National Institutes of Health Grant DK-42502 and an American Diabetes Association mentor award–based fellowship to M.A.M.

No potential conflicts of interest relevant to this article were reported.

Y.G. researched data and wrote, reviewed, and edited the article. J.L. researched data and contributed to discussion. W.Y. contributed to discussion and reviewed the article. A.K. contributed to discussion and reviewed the article. M.A.M. contributed to discussion and wrote, reviewed, and edited the article.

Parts of this study were presented in an oral session at the 69th Scientific Sessions of the American Diabetes Association, New Orleans, Louisiana, 5–9 June 2009.

The authors thank Dr. Maureen Gannon in the Department of Medicine at Vanderbilt University for many helpful discussions and proofreading the article, Leah Potter and Anna Osipovich in the Center for Stem Cell Biology at Vanderbilt University for helpful suggestions, and Alisha Mendonsa and Yi Xiao at Vanderbilt University for performing cell morphometry.

REFERENCES

1. Terauchi Y, Takamoto I, Kubota N, et al. Glucokinase and IRS-2 are required for compensatory beta cell hyperplasia in response to high-fat diet-induced insulin resistance. J Clin Invest 2007;117:246–257
2. Bishop JD, Nien WL, Dauphinee SM, Too CK. Prolactin activates mammalian target-of-rapamycin through phosphatidylinositol 3-kinase and stimulates phosphorylation of p70S6K and 4E-binding protein-1 in lymphoma cells. J Endocrinol 2006;190:307–312
3. Heit JJ, Karnik SK, Kim SK. Intrinsic regulators of pancreatic beta-cell proliferation. Annu Rev Cell Dev Biol 2006;22:311–338
4. Stiles BL, Kuralwalla-Martinez C, Guo W, et al. Selective deletion of Pten in pancreatic beta cells leads to increased islet mass and resistance to STZ-induced diabetes. Mol Cell Biol 2006;26:2772–2781
5. Tuttle RL, Gill NS, Pugh W, et al. Regulation of pancreatic beta-cell growth and survival by the serine/threonine protein kinase Akt1/PKBalpha. Nat Med 2001;7:1133–1137
6. Withers DJ, Gutierrez JS, Towery H, et al. Disruption of IRS-2 causes type 2 diabetes in mice. Nature 1998;391:900–904
7. Hashimoto N, Kido Y, Uchida T, et al. Ablation of PDK1 in pancreatic beta cells induces diabetes as a result of loss of beta cell mass. Nat Genet 2006;38:589–593
8. Franke TF. PI3K/Akt: getting it right matters. Oncogene 2008;27:6473–6488
9. Marone R, Cmiljanovic V, Giese B, Wymann MP. Targeting phosphoinositide 3-kinase: moving towards therapy. Biochim Biophys Acta 2008;1784:159–185
10. Bhaskar PT, Hay N. The two TORCs and Akt. Dev Cell 2007;12:487–502
11. Guertin DA, Stevens DM, Thoreen CC, et al. Ablation in mice of the mTORC components raptor, rictor, or mLST8 reveals that mTORC2 is required for signaling to Akt-FOXO and PKCalpha, but not S6K1. Dev Cell 2006;11:859–871
12. Yang Q, Inoki K, Ikenoue T, Guan KL. Identification of Sin1 as an essential TORC2 component required for complex formation and kinase activity. Genes Dev 2006;20:2820–2832
13. Dickson LM, Rhodes CJ. Pancreatic beta-cell growth and survival in the onset of type 2 diabetes: a role for protein kinase B in the Akt? Am J Physiol Endocrinol Metab 2004;287:E192–E198
14. Teta M, Long SY, Wartschow LM, Rankin MM, Kushner JA. Very slow turnover of beta-cells in aged adult mice. Diabetes 2005;54:2557–2567
15. Ackermann Misfeldt A, Costa RH, Gannon M. Beta-cell proliferation, but not neogenesis, following 60% partial pancreatectomy is impaired in the absence of FoxM1. Diabetes 2008;57:3069–3077
16. Brissova M, Shiota M, Nicholson WE, et al. Reduction in pancreatic transcription factor PDX-1 impairs glucose-stimulated insulin secretion. J Biol Chem 2002;277:11225–11232
17. Wang T, Lacík I, Brissová M, et al. An encapsulation system for the immunoisolation of pancreatic islets. Nat Biotechnol 1997;15:358–362
18. Shiota C, Woo JT, Lindner J, Shelton KD, Magnuson MA. Multiallelic disruption of the rictor gene in mice reveals that mTOR complex 2 is essential for fetal growth and viability. Dev Cell 2006;11:583–589
19. Rhodes CJ. Type 2 diabetes-a matter of beta-cell life and death? Science 2005;307:380–384
20. Ackermann AM, Gannon M. Molecular regulation of pancreatic beta-cell mass development, maintenance, and expansion. J Mol Endocrinol 2007;38:193–206
21. Zhong L, Georgia S, Tschen SI, Nakayama K, Nakayama K, Bhushan A. Essential role of Skp2-mediated p27 degradation in growth and adaptive expansion of pancreatic beta cells. J Clin Invest 2007;117:2869–2876
22. Kitamura T, Nakae J, Kitamura Y, et al. The forkhead transcription factor Foxo1 links insulin signaling to Pdx1 regulation of pancreatic beta cell growth. J Clin Invest 2002;110:1839–1847
23. Elrick LJ, Docherty K. Phosphorylation-dependent nucleocytoplasmic shuttling of pancreatic duodenal homeobox-1. Diabetes 2001;50:2244–2252
24. Nlend RN, Michon L, Bavamian S, et al. Connexin36 and pancreatic beta-cell functions. Arch Physiol Biochem 2006;112:74–81
25. Speier S, Gjinovci A, Charollais A, Meda P, Rupnik M. Cx36-mediated coupling reduces beta-cell heterogeneity, confines the stimulating glucose concentration range, and affects insulin release kinetics. Diabetes 2007;56:1078–1086
26. Hou JC, Min L, Pessin JE. Insulin granule biogenesis, trafficking and exocytosis. Vitam Horm 2009;80:473–506
27. Johnson JD, Bernal-Mizrachi E, Alejandro EU, et al. Insulin protects islets from apoptosis via Pdx1 and specific changes in the human islet proteome. Proc Natl Acad Sci U S A 2006;103:19575–19580
28. Wu H, MacFarlane WM, Tadayyon M, Arch JR, James RF, Docherty K. Insulin stimulates pancreatic-duodenal homoeobox factor-1 (PDX1) DNA-binding activity and insulin promoter activity in pancreatic beta cells. Biochem J 1999;344:813–818
29. Buzzi F, Xu L, Zuellig RA, et al. Differential effects of protein kinase B/Akt isoforms on glucose homeostasis and islet mass. Mol Cell Biol 2010;30:601–612
30. Georgia S, Bhushan A. Beta cell replication is the primary mechanism for maintaining postnatal beta cell mass. J Clin Invest 2004;114:963–968

31. Nakae J, Biggs WH 3rd, Kitamura T, et al. Regulation of insulin action and pancreatic beta-cell function by mutated alleles of the gene encoding forkhead transcription factor Foxo1. Nat Genet 2002;32:245–253
32. Westmoreland JJ, Wang Q, Bouzaffour M, Baker SJ, Sosa-Pineda B. Pdk1 activity controls proliferation, survival, and growth of developing pancreatic cells. Dev Biol 2009;334:285–298
33. Chalhoub N, Zhu G, Zhu X, Baker SJ. Cell type specificity of PI3K signaling in Pdk1- and Pten-deficient brains. Genes Dev 2009;23:1619–1624
34. Haga S, Ozaki M, Inoue H, et al. The survival pathways phosphatidylinositol-3 kinase (PI3-K)/phosphoinositide-dependent protein kinase 1 (PDK1)/Akt modulate liver regeneration through hepatocyte size rather than proliferation. Hepatology 2009;49:204–214
35. Mora A, Davies AM, Bertrand L, et al. Deficiency of PDK1 in cardiac muscle results in heart failure and increased sensitivity to hypoxia. EMBO J 2003;22:4666–4676
36. Mora A, Lipina C, Tronche F, Sutherland C, Alessi DR. Deficiency of PDK1 in liver results in glucose intolerance, impairment of insulin-regulated gene expression and liver failure. Biochem J 2005;385:639–648
37. Lawlor MA, Mora A, Ashby PR, et al. Essential role of PDK1 in regulating cell size and development in mice. EMBO J 2002;21:3728–3738
38. Rachdi L, Balcazar N, Osorio-Duque F, et al. Disruption of Tsc2 in pancreatic beta cells induces beta cell mass expansion and improved glucose tolerance in a TORC1-dependent manner. Proc Natl Acad Sci U S A 2008; 105:9250–9255
39. Hamada S, Hara K, Hamada T, et al. Upregulation of the mammalian target of rapamycin complex 1 pathway by Ras homolog enriched in brain in pancreatic beta-cells leads to increased beta-cell mass and prevention of hyperglycemia. Diabetes 2009;58:1321–1332
40. Wullschleger S, Loewith R, Hall MN. TOR signaling in growth and metabolism. Cell 2006;124:471–484